CERN-PH-2018-YYY
November 28, 2018

HL/HE-LHC Physics Workshop Report
WG3 : Beyond the Standard Model Physics

Editors:
X. Cid-Vidal[1], *M. D'Onofrio*[2], *P.J. Fox*[3], *R. Torre*[4,5], *K. Ulmer*[6],

Contributors:
A. Aboubrahim[7], *B. Allanach*[8], *M. Altakach*[9], *J.Y. Araz*[10], *A. Arbey*[11,12], *H. Baer*[13], *M.J. Baker*[13], *D. Barducci*[14], *V. Barger*[13], *M. Battaglia*[15,12], *D. Bhatia*[16], *S. Biswas*[17], *D. Buttazzo*[18], *G. Cacciapaglia*[19], *D.A. Camargo*[20], *A. Chakraborty*[13], *S.V. Chekanov*[21], *J.T. Childers*[21], *G. Corcella*[22], *S.D. Curtis*[23], *A. Deandrea*[24], *R. Dermisek*[25], *G. Ferretti*[26], *T. Flacke*[27], *M. Frank*[10], *D. Frizzell*[28], *E. Fuchs*[29], *B. Fuks*[30,31], *E. Gabrielli*[4,32,33], *J. Gainer*[13], *B. Gripaios*[34], *B.S.E. Haghi*[35], *U. Haisch*[36,37], *T. Han*[35,38], *M. Heikinheimo*[39], *S. Heinemeyer*[13], *C. Helsens*[13], *K. Huitu*[39], *A. Ismail*[35], *A. Iyer*[24], *D. Jamin*[13], *T. Jezo*[40], *J. Kalinowski*[41], *Y.G. Kim*[42], *M. Klasen*[43], *M.D. Klimek*[44,45], *W. Kotlarski*[46], *S. Kuttimalai*[13], *I. Lewis*[47], *T. Li*[48,49], *S.H. Lim*[13], *Z. Liu*[50,51], *M. Low*[52], *E. Lunghi*[25], *F. Mahmoudi*[11,12], *M.L. Mangano*[13], *X. Marcano*[53], *A. Mariotti*[54], *M. McDonald*[55], *B. Mele*[56], *S. Mondal*[39], *M. Mondragon*[13], *S. Moretti*[57], *S. Moretti*[57,58], *S. Mukhopadhyay*[59,60], *P. Nath*[7], *M.M. Nojiri*[13], *O. Panella*[61], *P. Pani*[62], *L. Panizzi*[63], *C.B. Park*[64], *S. Pascoli*[65], *A. Pierce*[13], *G. Polesello*[66], *M. Presilla*[67,68], *J. Proudfoot*[21], *F.S. Queiroz*[20], *S.K. Rai*[69], *D. Redigolo*[52,70], *T. Rizzo*[13], *L.D. Rose*[71], *L.D. Rose*[23], *R. Ruiz*[65], *F. Sala*[72], *I. Schienbein*[9], *M. Schlaffer*[29], *M. Selvaggi*[13], *D. Sengupta*[13], *H. Serce*[13], *H. Serodio*[73], *B. Shakya*[13], *S. Shin*[74,75], *X. Tata*[13], *A. Tesi*[76], *A. Tesi*[23], *A. Thamm*[13], *K. Tobioka*[77], *F. Ungaro*[55], *H. Waltari*[39,78], *X. Wang*[59], *R. Wang*[21], *C. Weiland*[65], *K. Yagyu*[23,79], *T.T. You*[80], *G. Zoupanos*[13]

[1] Instituto Galego de Física de Altas Enerxías (IGFAE), Universidade de Santiago de Compostela, Santiago de Compostela, Spain
[2] Oliver Lodge Laboratory, University of Liverpool, Liverpool, United Kingdom
[3] Theoretical Physics Department, Fermi National Accelerator Laboratory, Batavia, Illinois, 60510, USA
[4] Theoretical Physics Department, CERN, Geneva, Switzerland
[5] INFN Sezione di Genova, Via Dodecaneso 33, 16146 Genova, Italy
[6] University of Colorado Boulder, Boulder, USA

[7] Department of Physics, Northeastern University, Boston, MA 02115-5000, USA
[8] DAMTP, University of Cambridge, CMS, Wilberforce Road, Cambridge, CB3 0WA, United Kingdom
[9] Laboratoire de Physique Subatomique et de Cosmologie, Université Grenoble Alpes, CNRS/IN2P3, 53 Avenue des Martyrs, F-38026 Grenoble, France
[10] Department of Physics, Concordia University, 7141 Sherbrooke St.West, Montreal, QC, Canada H4B 1R6
[11] Univ. Lyon, Univ. Lyon 1, CNRS/IN2P3, Institut de Physique Nucléaire de Lyon, UMR5822, F-69622 Villeurbanne, France
[12] CERN, CH-1211 Geneva 23, Switzerland
[13] UNKNOWN
[14] SISSA and INFN, Sezione di Trieste, via Bonomea 265, 34136 Trieste, Italy
[15] University of California at Santa Cruz, Santa Cruz Institute of Particle Physics, CA 95064, USA
[16] Department of Theoretical Physics, Tata Institute of Fundamental Research, Homi Bhabha Road, Colaba, Mumbai 400 005, India
[17] Department of Physics, Ramakrishna Mission Vivekananda University, Belur Math, Howrah - 711202, West Bengal
[18] INFN, sezione di Pisa, Largo Pontecorvo 3, I-56127 Pisa, Italy
[19] Université de Lyon, France; Université Lyon 1, CNRS/IN2P3, UMR5822 IPNL, F-69622 Villeurbanne Cedex, France
[20] International Institute of Physics, Universidade Federal do Rio Grande do Norte, Campus Universitario, Lagoa Nova, Natal-RN 59078-970, Brazil
[21] HEP Division, Argonne National Laboratory, 9700 S. Cass Avenue, Argonne, IL 60439, USA
[22] INFN, Laboratori Nazionali di Frascati, Via E. Fermi 40, I-00044, Frascati (RM), Italy
[23] INFN, Sezione di Firenze, and Department of Physics and Astronomy, University of Florence, Via G. Sansone 1, 50019 Sesto Fiorentino, Italy
[24] INFN-Sezione di Napoli, Via Cintia, 80126 Napoli, Italia
[25] Physics Department, Indiana University, Bloomington, IN 47405, USA
[26] Department of Physics, Chalmers University of Technology, Fysikgården, 41296 Göteborg, Sweden
[27] Center for Theoretical Physics of the Universe, Institute for Basic Science (IBS), Daejeon, 34126, Korea
[28] Homer L. Dodge Department of Physics and Astronomy, University of Oklahoma, Norman, OK, USA
[29] Department of Particle Physics and Astrophysics, Weizmann Institute of Science, 7610001 Rehovot, Israel
[30] Sorbonne Université, CNRS, Laboratoire de Physique Théorique et Hautes Energies, LPTHE, F-75005 Paris, France
[31] Institut Universitaire de France, 103 boulevard Saint-Michel, 75005 Paris, France
[32] Dipart. di Fisica Teorica, Università di Trieste, Strada Costiera 11, I-34151 Trieste
[33] INFN, Sezione di Trieste, Via Valerio 2, I-34127 Trieste, Italy
[34] Cavendish Laboratory, JJ Thomson Ave, University of Cambridge, CB3 0HE, United Kingdom
[35] PITT-PACC, Department of Physics and Astronomy, University of Pittsburgh, Pittsburgh, PA 15260, USA
[36] Rudolf Peierls Centre for Theoretical Physics, University of Oxford, OX1 3NP Oxford, United Kingdom
[37] CERN, Theoretical Physics Department, CH-1211 Geneva 23, Switzerland
[38] Department of Physics, Tsinghua University, and Collaborative Innovation Center of Quantum Matter, Beijing, 100086, China
[39] Department of Physics and Helsinki Institute of Physics, University of Helsinki, P.O. Box 64 (Gustaf Hällströmin katu 2), FI-00014 University of Helsinki, Finland
[40] Physics Institute, Universität Zürich, Zürich, Switzerland

[41] Faculty of Physics, University of Warsaw, Warsaw, Poland
[42] Department of Science Education, Gwangju National University of Education, Gwangju 61204, Korea
[43] Institut für Theoretische Physik, Westfälische Wilhelms-Universität Münster, Wilhelm-Klemm-Straße 9, D-48149, Münster, Germany
[44] Laboratory for Elementary Particle Physics, Cornell University, Ithaca, NY 14853, USA
[45] Department of Physics, Korea University, Seoul 02841, Republic of Korea
[46] Institut fuer Kern- und Teilchenphysik, TU Dresden, Dresden, Germany
[47] Department of Physics and Astronomy, University of Kansas, Lawrence, KS 66045, USA
[48] School of Physics, Nankai University, Tianjin 300071, China
[49] ARC Centre of Excellence for Particle Physics at the Terascale, School of Physics and Astronomy, Monash University, Melbourne, Victoria 3800, Australia
[50] Theoretical Physics Department, Fermi National Accelerator Laboratory, Batavia, IL, 60510
[51] Maryland Center for Fundamental Physics, Department of Physics, University of Maryland, College Park, MD 20742, USA
[52] School of Natural Sciences, Institute for Advanced Study, Einstein Drive, Princeton, NJ 08540, USA
[53] Laboratoire de Physique Théorique, CNRS, Univ. Paris-Sud, Université Paris-Saclay, 91405 Orsay, France
[54] Theoretische Natuurkunde and IIHE/ELEM, Vrije Universiteit Brussel, and International, Solvay Institutes, Pleinlaan 2, B-1050 Brussels, Belgium
[55] The School of Physics, University of Melbourne, Victoria, Australia
[56] INFN, Sezione di Roma, P. le A. Moro 2, I-00185 Rome, Italy
[57] School of Physics and Astronomy, University of Southampton, Highfield, Southampton SO17 1BJ, United Kingdom
[58] Particle Physics Department, Rutherford Appleton Laboratory, Chilton, Didcot, Oxon OX11 0QX, United Kingdom
[59] PITT-PACC, Department of Physics and Astronomy, University of Pittsburgh, PA 15260, USA
[60] Department of Theoretical Physics, Indian Association for the Cultivation of Science, Kolkata 700032, India
[61] INFN, Istituto Nazionale di Fisica Nucleare, Sezione di Perugia, Via A. Pascoli, 06123, Perugia
[62] CERN, Experimental Physics Department, CH-1211 Geneva 23, Switzerland
[63] Dipartimento di Fisica, Università di Pisa and INFN, Sezione di Pisa, Largo Pontecorvo 3, I-56127 Pisa, Italy
[64] Center for Theoretical Physics of the Universe, Institute for Basic Science (IBS), Daejeon 34051, Korea
[65] Institute for Particle Physics Phenomenology (IPPP), Department of Physics, Durham University, Durham, DH1 3LE, UK
[66] INFN, Sezione di Pavia Via Bassi 6, 27100 Pavia, Italy
[67] Dipartimento di Fisica e Astronomia "Galileo Galielei", Università degli Studi di Padova, Via Marzolo, I-35131, Padova, Italy
[69] Regional Centre for Accelerator-based Particle Physics, Harish-Chandra Research Institute, HBNI, Chhatnag Road, Jhusi, Allahabad 211019, India
[70] Raymond and Beverly Sackler School of Physics and Astronomy, Tel-Aviv University, Tel-Aviv 69978, Israel
[71] INFN, Sezione di Firenze, and Dipartimento di Fisica ed Astronomia, Università di Firenze, Via G. Sansone 1, 50019 Sesto Fiorentino, Italy
[72] DESY, Notkestraße 85, D-22607 Hamburg, Germany
[73] Department of Astronomy and Theoretical Physics, Lund University, SE-223 62 Lund, Sweden
[74] Enrico Fermi Institute, University of Chicago, Chicago, IL 60637, USA
[75] Department of Physics & IPAP, Yonsei University, Seoul 03722, Korea

[76] INFN, sezione di Firenze, Via G. Sansone 1, I-59100 Sesto F.no, Italy
[77] C.N. Yang Institute for Theoretical Physics, Stony Brook University, Stony Brook, NY 11794-3800
[78] Department of Physics and Astronomy, University of Southampton, Highfield, Southampton SO17 1BJ, United Kingdom
[79] Seikei University, Musashino, Tokyo 180-8633, Japan
[80] Gonville and Caius College, University of Cambridge, Trinity Street, CB2 1TA, United Kingdom

Abstract

Contents

Some global fixes still missing:

- Notation to refer to the panels of figures: right vs right-hand, top vs upper etc.
- Should we replace everywhere the ugly 3000 fb^{-1} with 3 ab^{-1}?
- We have to uniform notation for MET, PT, KT and all kinematic variables in general;
- For the sections where paragraphs or subsubsections remain uniform the notation;

1 Other BSM signatures

1.1 Spin 0 and 2 resonances

1.2 Spin 1 resonances

*1.2.1 High mass dilepton searches at HE-LHC (ee, $\mu\mu$, $\tau\tau$) [TH]**

Contribution from: C. Helsens, D. Jamin, M. Selvaggi(RT)

RT: There are comments to address.

Models with extended gauge groups often feature additional U(1) symmetries with corresponding heavy spin-1 bosons. These bosons, generally referred to as Z', would manifest themselves as a narrow resonance in the dilepton invariant mass spectrum. Among these models are those inspired by Grand Unified Theories, motivated by gauge unification, or a restoration of the left-right symmetry violated by the weak interaction. Examples include the Z' bosons of the E_6 motivated theories [1–3] and Minimal models [4]. The Sequential Standard Model (SSM) [3] posits a $Z'_{\rm SSM}$ boson with couplings to fermions that are identical to those of the Standard Model Z boson.

The decay products of heavy resonances are in the multi-TeV regime and the capability to reconstruct their momentum imposes stringent requirement on the detector design. In particular, reconstructing the track curvature of multi-TeV muons requires excellent position resolution and a large lever arm. In this section, the expected sensitivity is presented for a $Z' \to \ell\ell$ (where $\ell = {\rm e}, \mu$) and $Z' \to \tau\tau$ separately.

Monte Carlo simulated event samples were used to simulate the response of the future detector to signal and backgrounds. The muon momentum resolution is assumed to be $\sigma(p)/p \approx 10\%$ at $p_T = 5$ TeV for central muons. Signals are generated with PYTHIA 8.230 [5] using the leading order cross-section from the generator. All lepton flavour decays of the $Z'_{\rm SSM}$ are generated assuming universality of the couplings. The Drell-Yan background has been generated using MADGRAPH5_aMC@NLO 2.5.2 [6] at leading order only. A conservative overall k-factor of 2 has been applied to all the background processes to account for possible higher order QCD corrections.(RT)

RT: In every contribution you put a k-factor of 2 on the background. This seems an irrelevant arbitrary assumption.

For the $\ell\ell$ final-states events are required to contain two isolated leptons with $p_T > 500$ GeV and $|\eta| < 4$. For the $\tau\tau$ final state we focus solely on the fully hadronic decay mode which is expected to drive the sensitivity. The $\tau\tau$ event selection requires the presence two reconstrcuted jets with $p_T > 500$ GeV and $|\eta| < 2.5$ identified as hadronic τ's. To ensure orthogonality between the ℓ and τ final states, jets overlapping with isolated leptons are vetoed. Additionnal mass dependent selection criteria on the azimutal angle between the two reconstructed τ's are applied to further improve the QCD background rejection (see table 1).

The left and central panels of fig. 1 show the invariant mass distribution for a 6 TeV $Z'_{\rm SSM}$ in the ee and $\mu\mu$ channels. The mass resolution is better for the ee channel, as expected. The right panel of fig. 1 shows the transverse mass [1] of a 6 TeV signal for the $\tau\tau$ channel. Because of the presence of neutrinos in τ decays, the true resonance mass cannot be reconstructed. Several arbitrary choices are possible to approximate the Z' mass. The transverse mass provided the best sensitivity and was therefore used to set limits and determine the discovery reach in $\tau\tau$ decay mode.

Hypothesis testing is performed using a modified frequentist method based on a profile likelihood that takes into account the systematic uncertainties as nuisance parameters that are fitted to the expected

[1] The transverse mass is defined as $m_T = \sqrt{2p_{\rm T}^{Z'} * E_{\rm T}^{\rm miss} * (1 - \cos\Delta\phi(Z', E_{\rm T}^{\rm miss}))}$.

Z' mass [TeV]	$\Delta\phi(\tau_1,\tau_2)$	$\Delta R(\tau_1,\tau_2)$	$E_{\mathrm{T}}^{\mathrm{miss}}$
2	> 2.4	> 2.4 and < 3.9	> 80 GeV
4	> 2.4	> 2.7 and < 4.4	> 80 GeV
6	> 2.4	> 2.9 and < 4.4	> 80 GeV
8	> 2.6	> 2.9 and < 4.6	> 80 GeV
10	> 2.8	> 2.9 and < 4.1	> 60 GeV
12	> 2.8	> 3.0 and < 3.6	> 60 GeV
14	> 3.0	> 3.0 and < 3.3	> 60 GeV

Table 1: List of mass dependent cuts optimised to maximise the sensitivity for the $Z' \to \tau\tau$ search.

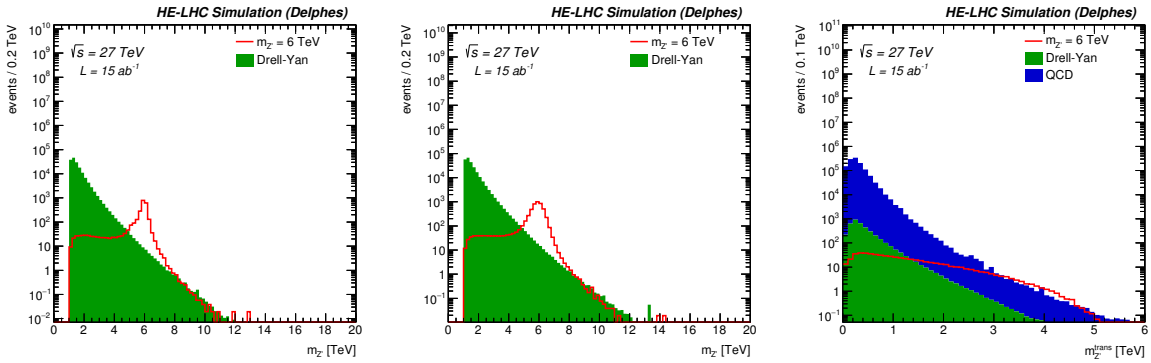

Fig. 1: Left, center: Invariant mass for a 6 TeV signal after full event selection for ee channel (left) and $\mu\mu$ channel (center). Right: Transverse mass for a 6 TeV signal after full event selection for the $\tau\tau$ channel.

background predicted from Monte Carlo. For the ee and $\mu\mu$ analyses, the dilepton invariant mass is used as the discriminant, while for the $\tau\tau$ channel the transverse mass is used. A 50% uncertainty on the background normalisation is assumed.

The 95% C.L. exclusion limit obtained using $\mathcal{L} = 15$ ab^{-1} of data for the combination of the ee and $\mu\mu$ channels is shown in fig. 2 (left) for a list of 6 different Z' models. A detailed discussion on model discrimination at HE-LHC following the observation of an excess at the HL-LHC can be found in Section 1.2.2. We simply note here that it is possible to exlude a Z' with $m_{Z'} \lesssim 10-12$ TeV (depending on the model) at $\sqrt{s} = 27$ TeV with $\mathcal{L} = 15$ ab^{-1}. Figure 2 (right) shows the integrated luminosity required to reach a 5σ discovery for a Z'_{SSM} decaying leptonically as a function of the mass of the heavy resonance. Despite a worse di-lepton invariant mass resolution for the $\mu\mu$ final state, the $Z' \to ee$ and $Z' \to \mu\mu$ channel display very similar performances, due to the low background rates and a higher muon reconstruction efficiency. With the full dataset $\mathcal{L} = 15$ ab^{-1}, a Z'_{SSM} up to $m_{Z'} \approx 13$ TeV can be discovered. Figure 3 shows the exclusion limits for 15 ab^{-1} of data (left) and the required integrated luminosity versus mass to reach a 5σ discovery (right) for the $\tau\tau$ resonances. We find that a Z'_{SSM} with $m_{Z'} \approx 6.5$ TeV can be discovered or excluded. As expected, the $Z' \to \tau\tau$ final-state yields to a worse discovery potential compared to the $\ell\ell$ final states because of the presence of a much larger background contribution as well as the absence of narrow mass peak.

*1.2.2 Z' discrimination at HE-LHC in case of an evidence/discovery after HL-LHC [TH]**

Contribution from: C. Helsens, D. Jamin, M. L. Mangano, T. Rizzo, M. Selvaggi

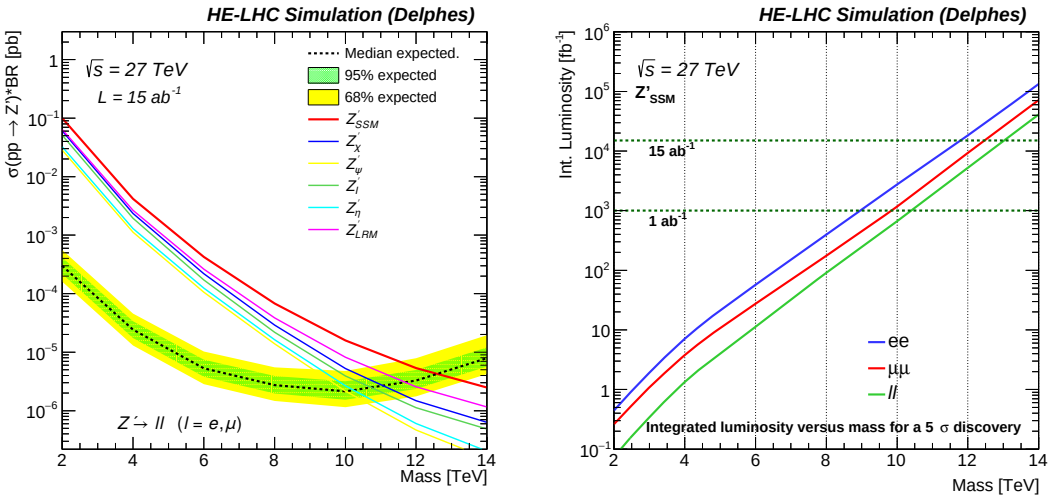

Fig. 2: Exclusion limit versus mass for the dilepton (ee,$\mu\mu$) channel (left) and luminosity for a 5σ discovery (right) comparing ee,$\mu\mu$ and combined channels.

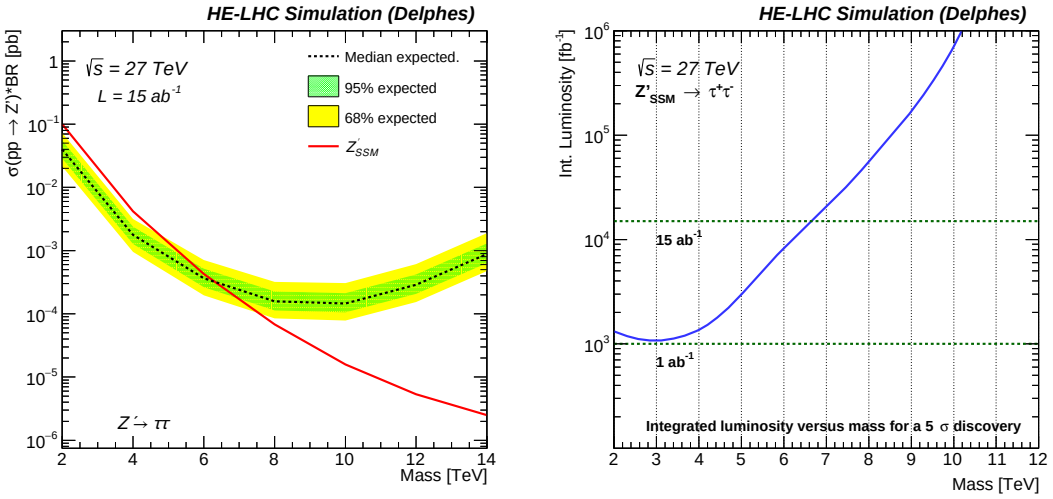

Fig. 3: Exclusion Limit versus mass for the ditau channel (left) and luminosity for a 5σ discovery (right).

Context of the study

It is legitimate to assume that a heavy resonance could be seen at the end of HL-HLC. If that is the case a new collider with higher energy in the c.o.m. is needed to study its properties as too few events will be available at $\sqrt{s} = 14$ TeV. In this document we present the discrimination potential of a High Energy LHC (HE-LHC) with an assumed c.o.m. energy of 27 TeV. Here we analyzed the capability of the $\sqrt{s} = 27$ TeV HE-LHC with $\mathcal{L} = 15$ ab^{-1} to distinguish among six Z' models. Under the assumption that these Z''s decay only to SM particles, we show that there are sufficient observables to perform this model differentiation in most cases.

Bounds from HL-LHC

As a starting point it is needed to understand what are, for $\sqrt{s} = 14$ TeV, for the typical exclusion/discovery reaches for some standard reference Z' models assuming $\mathcal{L} = 3$ ab^{-1} employing only the e^+e^- and $\mu^+\mu^-$ channels. To address this and the other questions below we will use the same set of

Model	95% C.L.	3σ	5σ
SSM	6.62	6.09	5.62
LRM	6.39	5.85	5.39
ψ	6.10	5.55	5.07
χ	6.22	5.68	5.26
η	6.15	5.59	5.16
I	5.98	5.45	5.05

Table 2: Mass reach for several Z' models at $\sqrt{s} = 14$ TeV with $\mathcal{L} = 3$ ab^{-1}.

Z' models as employed in Ref. [7] and mostly in Ref. [8], both of which we will refer to frequently. We employ the MMHT2014 NNLO PDF set [9] throughout with an appropriate constant K-factor (=1.27) to account for higher order QCD corrections. The production cross section times leptonic branching fraction is shown in Figure 4 (left) for these models at $\sqrt{s} = 14$ TeV in the narrow width approximation (NWA). It has been and will be assumed here that these Z' states only decay to SM particles.

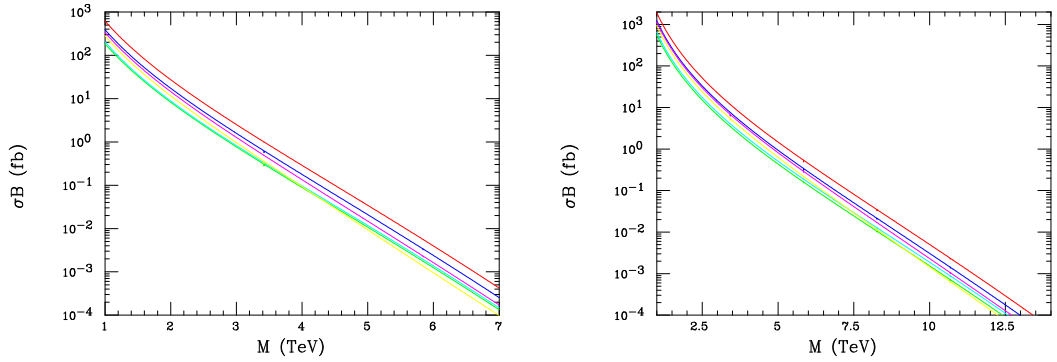

Fig. 4: Left: σB_l in the NWA for the Z' production at the $\sqrt{s} = 14$ TeV LHC as functions of the Z' mass: SSM(red), LRM (blue), ψ(green), χ(magenta), η(cyan), I(yellow). (Right) σB_l of Z' in models described in (left) at $\sqrt{s} = 27$ TeV.

Using the present ATLAS and CMS results at 13 TeV, [10] and [11], it is straightforward to estimate by extrapolation the exclusion reach at $\sqrt{s} = 14$ TeV using the combined $ee + \mu\mu$ final states. This is given in the first column of Table 2. For discovery, only the ee channel is used due to poor $\mu\mu$-pair invariant mass resolution near $M_{Z'} = 6$ TeV. Estimates of the 3σ evidence and 5σ discovery limits are also given in Table 2. Based on these results, we will assume in our study below that we are dealing with a Z' of mass 6 TeV. Figure 4 (right) shows the NWA cross sections for the same set of models but now at $\sqrt{s} = 27$ TeV with $\mathcal{L} = 15$ ab^{-1}. We note that very large statistical samples will be available for the case of $M_{Z'} = 6$ TeV for each dilepton channel.

Definition of the discriminating variables

The various Z' models can be disentangled with the help of 3 inclusive observables: the production cross section times leptonic branching fraction σB_l, the forward-backward asymmetry A_{FB} and the rapidity ratio r_y. The variable A_{FB} can be seen as an estimate of the charge asymmetry

$$A_{FB} = A_C = \frac{\sigma(\Delta|y| > 0) - \sigma(\Delta|y| < 0)}{\sigma(\Delta|y| > 0) + \sigma(\Delta|y| < 0)}, \tag{1}$$

where $\Delta|y| = |y_l| - |y_{\bar{l}}|$. It has been checked that this definition is equivalent to defining

$$A_{FB} = \frac{\sigma_F - \sigma_B}{\sigma_F + \sigma_B}, \tag{2}$$

with $\sigma_F = \sigma(cos\theta^*_{cs}) > 0$ and $\sigma_B = \sigma(cos\theta^*_{cs}) < 0$ where θ^*_{cs} is the Collins-Soper frame angle. The variable r_y is defined as the ratio of central over forward events:

$$r_y = \frac{\sigma(|y_{Z'}| < y_1)}{\sigma(y_1 < |y_{Z'}| < y_2)}, \tag{3}$$

where $y_1 = 0.5$ and $y_2 = 2.5$.

Model discrimination

The model discrimination presented in this section has been performed assuming the HE-LHC detector parametrisation [12] in DELPHES [13]. In such a detector, muons at $\eta \approx 0$ are assumed to be reconstructed with a resolution $\sigma(p)/p \approx 7\%$ for $p_T = 3$ TeV.

Leptonic final states The potential for discriminating various Z' models is first investigated using the leptonic ee and $\mu\mu$ final states only. The signal samples for the 6 models and the Drell-Yan backgrounds have been generated with PYTHIA 8.230 [5] assuming including the interference between the signal and background. The Z' decays assume lepton flavour universality. For a description of the event selection and a discussion of the discovery potential in leptonic final states for the list of Z' models being discussed here, the reader should refer to Section [**?**]. We simply point out here that with $\mathcal{L} = 15$ ab^{-1} , all Z' models with $m_{Z'} \lesssim 10$ TeV can be excluded at $\sqrt{s} = 27$ TeV.

Figure 5 (left) shows the correlated predictions for the A_{FB} and the rapidity ratio r_y observables defined previously for these six models given the above assumptions. Here we see that apart from a possible near degeneracy in models ψ and η, a reasonable Z' model separation is indeed achieved.

Using a profile likelihood technique, the signal strength μ, or equivalently, σB_l, can be fitted together with its corresponding error using the the di-lepton invariant mass shape. The quantity σB_l and its total estimated uncertainty is shown in Figure 5 (center) as a function of the integrated luminosity. The σB_l measurement seems to be able to resolve the degeneracy between the ψ and η models with $\mathcal{L} = 15$ ab^{-1}. It should be noted however that since the cross-section can easily be modified by an overall rescaling of the couplings, further handles will be needed for a convincing discrimination. (RT)

RT: in plot right FCC Simulation -> HE-LHC simulation. Plot style can also be improved, line instead of boxes in legends. Increase line thickness in for better visibility.

Hadronic final states Model discrimination can be improved by including an analysis involving three Z' addition hadronic final states: $t\bar{t}$, $b\bar{b}$ and $q\bar{q}$, where $q = u, d, c, s$. The sample production and event selection for the $t\bar{t}$, $q\bar{q}$ final states has been described to some extent in Section [**?**]. We simply remind here that the analysis involves requiring the presence of two central high p_T jets. In order to ensure complete orthogonality between the various final states jets are required to be tagged as follows. In the $Z' \to t\bar{t}$ analysis both jets should be *top-tagged*. For the $Z' \to b\bar{b}$ final state both jets are required to be *b-tagged* and we veto events containing at least one top-tagged jet. Finally, in the $Z' \to q\bar{q}$ analysis, we veto events that contain at least one b-tagged or top-tagged jet.

Figure 5 (right) summarise the discrimination potential in terms of fitted cross-section of the different models considering the three aforementionned hadronic decays, $t\bar{t}$, $b\bar{b}$ and $q\bar{q}$. An good overall discrimination among the various models can be achieved using all possible final states. We note however that the degeneracy between η and Ψ can only be partially resolved resolved at $\approx 1\,\sigma$ by exploiting the difference in $t\bar{t}$ yield.

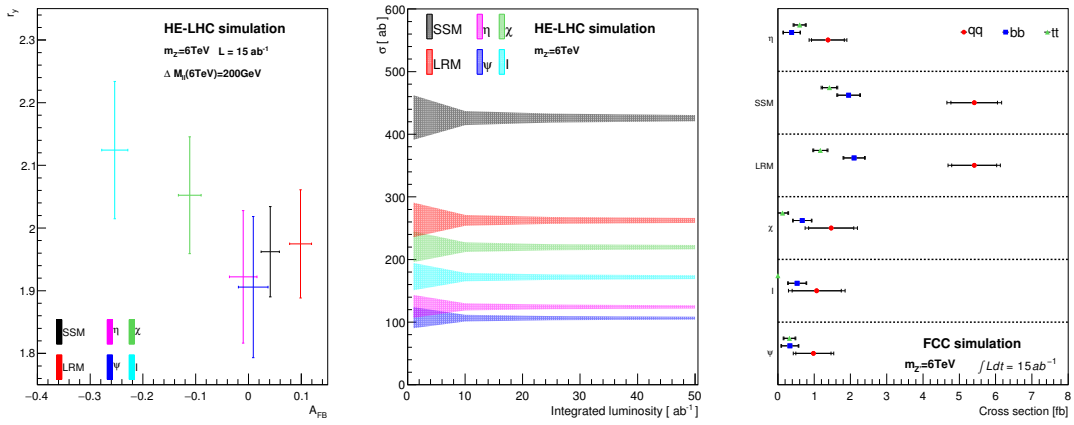

Fig. 5: Left: Scatter plot of r_y versus A_{FB} with 200 GeV and mass window. The full interference is included. Center: Fitted signal cross-section together with its corresponding error versus integrated luminosity. Right: Fitted cross-section of the three hadronic analyses. Statistical and full uncertainties are shown on each point.

Conclusion

1.3 Spin 1/2 resonances

1.4 Signature based analyses

*1.4.1 High mass resonance searches at HE-LHC using hadronic final states [TH]**

Contribution from: C. Helsens, D. Jamin, M. Selvaggi(RT)

RT: There are comments to address.

The presence of new resonant states [14–22] decaying to two highly boosted particles decaying hadronically could be observed as an excess in the invariant mass spectrum of two jets over the large SM background. In this section we present the reach at the HE-LHC for three distinct hadronic signatures: $Z' \to t\bar{t}$, $G_{RS} \to WW$ and $Q^* \to jj$. For the $Z' \to t\bar{t}$ decay mode the Sequential Standard Model $Z'_{\rm SSM}$ [3] and a leptophobic $Z'_{\rm TC2}$ [23, 24] have been considered as benchmarks Z'models. For the $G_{RS} \to WW$ and $Q^* \to jj$ decay modes, a Randall-Sundrum graviton [21] and excited heavy quarks [25, 26] have been taken as a benchmarks respectively.

The decay products of the heavy resonances are typically in the multi-TeV regime and their reconstruction imposes stringent requirement on the detector design. Precise jet energy resolution requires full longitudinal shower containment. Highly boosted W bosons and top quarks decay into highly collimated jets that need to be disentangled from standard QCD jets by characterizing their substructure. Thus, in order to achieve high sensitivity excellent granularity is needed both in the tracking detectors and in the calorimeters.

Signal events were generated at LO with PYTHIA 8.230 [5]. The considered SM backgrounds are dijet (QCD), top pairs ($t\bar{t}$), VV and $V+$ jets where $V = W/Z$, and were generated at LO using MADGRAPH5_aMC@NLO [6]. A conservative constant k-factor of 2 is applied to all the background processes to account for possible high order corrections(RT). The detector simulation was performed with DELPHES [13] assuming an HL-LHC generic detector [12].

RT: As in the other contributions this thing makes little sense to me.

An important ingredient of the $Z' \to t\bar{t}$ and $G_{RS} \to WW$ searches is the identification of hadronically decaying boosted tops and W bosons. To this end, a tagger using jet substructure observables was developed to discriminate W and top jets against QCD jets. It was found that jets using tracking only information (*track-jets*) feature better angular resolution compared to pure calorimeter based jets. Therefore, track-jets are the optimal choice to build jet substructure observables. The boosted top tagger is built from the following jet substructure observables: the soft-dropped jet mass [27] and N-subjettiness [28] variables $\tau_{1,2,3}$ and their ratios τ_2/τ_1 and τ_3/τ_2. In addition, the W-jet versus QCD-jet tagger also uses

an "isolation-like" variable that exploits the absence of high p_{T} final state-radiation (FSR) in the vicinity of the W decay products. Following the strategy defined in Ref. [29], we call these variables $E_{\mathrm{F}}(\mathrm{n},\alpha)$ and define them as:

$$E_{\mathrm{F}}(\mathrm{n},\alpha) = \frac{\sum\limits_{\frac{n-1}{5}\alpha<\Delta R(k,jet)<\frac{n}{5}\alpha} p_{\mathrm{T}}^{(k)}}{\sum\limits_{\Delta R(k,jet)<\alpha} p_{\mathrm{T}}^{(k)}} \tag{4}$$

We choose $\alpha = 0.05$, construct 5 variables $E_{\mathrm{F}}(\mathrm{n},\alpha)$with $n = 1..5$ and use them as input to the multivariate tagger. The W tagging performance has significantly better performance than the top-tagging due to the use of the energy-flow variables. We choose our working points with a top and W tagging efficiencies of $\epsilon_S^{\mathrm{top}} = 60\%$ and $\epsilon_S^{\mathrm{W}} = 90\%$ corresponding respectively to a background efficiency of $\epsilon_B^{\mathrm{top}} = \epsilon_B^{\mathrm{W}} = 10\%$.

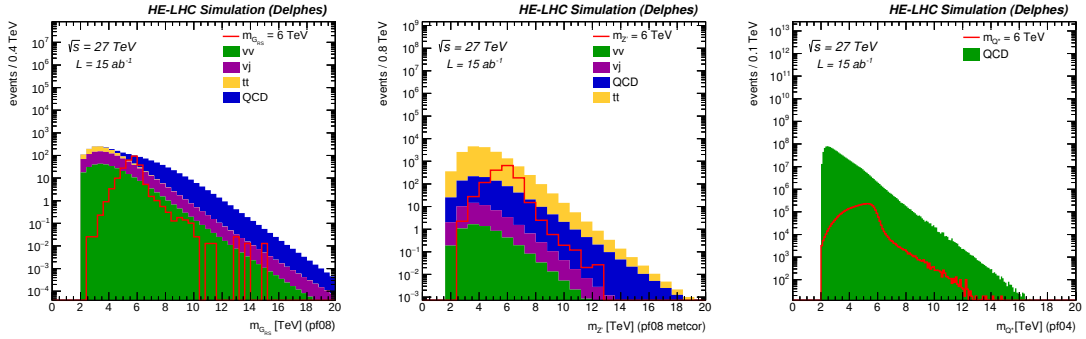

Fig. 6: Invariant mass distribution of the two selected jets for the full selection for a 6 TeV signal for the three benchmark analyses $Z' \to t\bar{t}$ (left), $G_{RS} \to WW$ (center) and $Q^* \to jj$ (right)

The event selection proceeds as follows: we require two jets with $p_{\mathrm{T}} > 1$ TeV, $|\eta| < 3$ and a small rapidity gap $\Delta\eta < 1.5$ between the two high p_{T} jets. For the $Z' \to t\bar{t}$ and $G_{RS} \to WW$ searches, the rapidity gap selection is relaxed to $\Delta\eta < 2.4$, both jets are required to be respectively top or W-tagged, and, to further reject background QCD jets, we require for both jets a large soft-dropped mass $m_{\mathrm{SD}} > 40$ GeV. Finally, for the $Z' \to t\bar{t}$ search alone, we require that both selected jets must also be b-tagged. Since no lepton veto is applied, there is also some acceptance for leptonic decays. The sensitivity to semi-leptonic $t\bar{t}$ decays is enhanced by adding the $\vec{p_{\mathrm{T}}}^{\,\mathrm{miss}}$ vector to the closest jet 4-momentum (among the two leading jets). The invariant mass of the two selected jets is used as a discriminant and is shown for the three benchmark analyses in Figure 6.

Hypothesis testing is performed using a modified frequentist method based on a profile likelihood fit that takes into account the systematic uncertainties (mostly the background normalisations) as nuisance parameters. The expected exclusion limit at 95% C.L. and discovery reach at 5 σ are shown in Figures 7 (top and bottom) for the various scenarios that have been considered. At $\sqrt{s} = 27$ TeV, and with an integrated luminosity $\mathcal{L} = 15$ ab^{-1}, it is possible to discover a G_{RS} up to $m_G \approx 7$ TeV, and to exclude $m_G \lesssim 8$ TeV. For the $Z' \to t\bar{t}$ search the exclusion reach is $m_{Z'} \lesssim 10(8.5)$ TeV and it is possible to discover it up to $m_{Z'} \approx 8(6.5)$ TeV for the TC2 and SSM models respectively. Finally, for the excited quark model, the exclusion reach is $m_{Q^*} \lesssim 14$TeV and the discovery reach is $m_{Q^*} \approx 12$TeV.

ADD FIGURE SUMMARY HELHC?

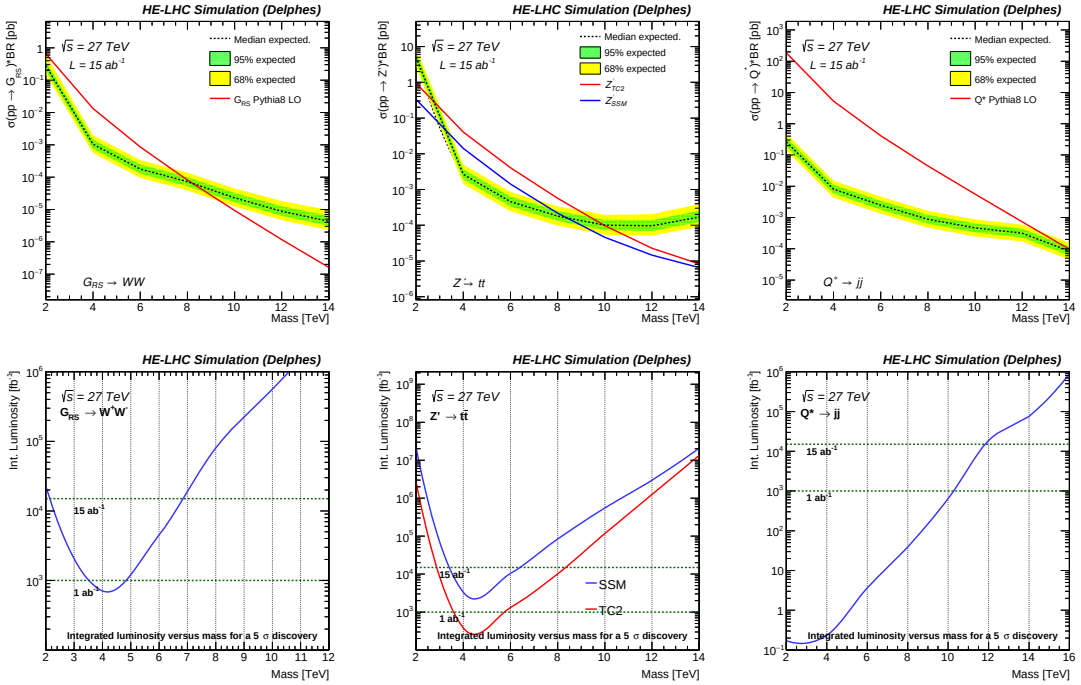

Fig. 7: Top: Exclusion limit at 95% C.L. versus heavy resonance mass for the three benchmark models: $Z' \to t\bar{t}$ (left), $G_{RS} \to WW$ (center) and $Q^* \to jj$ (right). Bottom: Integrated luminosity needed for a 5σ discovery as a function of the heavy resonance mass for the three benchmark models.

References

[1] D. London and J. L. Rosner, *Extra Gauge Bosons in E(6)*, in *Proceedings, 23RD International Conference on High Energy Physics, JULY 16-23, 1986, Berkeley, CA*. 1986.

[2] A. Joglekar and J. L. Rosner, *Searching for signatures of E_6*, Phys. Rev. **D96** (2017) no. 1, 015026, arXiv:1607.06900 [hep-ph].

[3] P. Langacker, *The Physics of Heavy Z' Gauge Bosons*, Rev. Mod. Phys. **81** (2009) 1199–1228, arXiv:0801.1345 [hep-ph].

[4] E. Salvioni, G. Villadoro, and F. Zwirner, *Minimal Z-prime models: Present bounds and early LHC reach*, JHEP **11** (2009) 068, arXiv:0909.1320 [hep-ph].

[5] T. Sjöstrand, S. Ask, J. R. Christiansen, R. Corke, N. Desai, P. Ilten, S. Mrenna, S. Prestel, C. O. Rasmussen, and P. Z. Skands, *An Introduction to PYTHIA 8.2*, Comput. Phys. Commun. **191** (2015) 159–177, arXiv:1410.3012 [hep-ph].

[6] J. Alwall, R. Frederix, S. Frixione, V. Hirschi, F. Maltoni, O. Mattelaer, H. S. Shao, T. Stelzer, P. Torrielli, and M. Zaro, *The automated computation of tree-level and next-to-leading order differential cross sections, and their matching to parton shower simulations*, JHEP **07** (2014) 079, arXiv:1405.0301 [hep-ph].

[7] T. G. Rizzo, *Exploring new gauge bosons at a 100 TeV collider*, Phys. Rev. **D89** (2014) no. 9, 095022, arXiv:1403.5465 [hep-ph].

[8] T. Han, P. Langacker, Z. Liu, and L.-T. Wang, *Diagnosis of a New Neutral Gauge Boson at the LHC and ILC for Snowmass 2013*, arXiv:1308.2738 [hep-ph].

[9] L. A. Harland-Lang, A. D. Martin, P. Motylinski, and R. S. Thorne, *Parton distributions in the LHC era: MMHT 2014 PDFs*, Eur. Phys. J. C **75** (2015) 204, arXiv:1412.3989 [hep-ph].

[10] ATLAS Collaboration, ATLAS Collaboration, *Search for new high-mass phenomena in the dilepton final state using 36.1 fb^{-1} of proton-proton collision data at $\sqrt{s}$ = 13 TeV with the ATLAS*

detector, JHEP **10** (2017) 182, arXiv:1707.02424 [hep-ex].

[11] CMS Collaboration, A. M. Sirunyan et al., *Search for high-mass resonances in dilepton final states in proton-proton collisions at* $\sqrt{s} = 13$ *TeV*, arXiv:1803.06292 [hep-ex].

[12] *High Energy LHC main page*, 2018. https://twiki.cern.ch/twiki/bin/view/LHCPhysics/HLHELHCWorkshop.

[13] DELPHES 3 Collaboration, J. de Favereau, C. Delaere, P. Demin, A. Giammanco, V. Lemaître, A. Mertens, and M. Selvaggi, *DELPHES 3, A modular framework for fast simulation of a generic collider experiment*, JHEP **02** (2014) 057, arXiv:1307.6346 [hep-ex].

[14] R. M. Harris and K. Kousouris, *Searches for Dijet Resonances at Hadron Colliders*, Int. J. Mod. Phys. **A26** (2011) 5005–5055, arXiv:1110.5302 [hep-ex].

[15] N. Boelaert and T. Akesson, *Dijet angular distributions at* $s^{1/2}$ *=14 TeV*, Eur. Phys. J. **C66** (2010) 343–357, arXiv:0905.3961 [hep-ph].

[16] T. D. Lee, *A Theory of Spontaneous T Violation*, Phys. Rev. **D8** (1973) 1226–1239. [,516(1973)].

[17] G. C. Branco, P. M. Ferreira, L. Lavoura, M. N. Rebelo, M. Sher, and J. P. Silva, *Theory and phenomenology of two-Higgs-doublet models*, Phys. Rept. **516** (2012) 01, arXiv:1106.0034 [hep-ph].

[18] C. T. Hill, *Topcolor assisted technicolor*, Phys. Lett. **B345** (1995) 483–489, arXiv:hep-ph/9411426 [hep-ph].

[19] D. B. Kaplan, H. Georgi, and S. Dimopoulos, *Composite Higgs Scalars*, Phys. Lett. **136B** (1984) 187–190.

[20] Brando Bellazzini and Csaba Csáki and Javi Serra, *Composite Higgses*, Eur. Phys. J. **C74** (2014) no. 5, 2766, arXiv:1401.2457 [hep-ph].

[21] L. Randall and R. Sundrum, *A large mass hierarchy from a small extra dimension*, Phys. Rev. Lett. **83** (1999) 3370, arXiv:hep-ph/9905221 [hep-ph].

[22] A. Pomarol, *Gauge bosons in a five-dimensional theory with localized gravity*, Phys. Lett. **B486** (2000) 153–157, arXiv:hep-ph/9911294 [hep-ph].

[23] R. M. Harris, C. T. Hill, and S. J. Parke, *Cross-Section for Topcolor* Z'_t *Decaying to* $t\bar{t}$, arXiv:hep-ph/9911288 [hep-ph].

[24] R. M. Harris and S. Jain, *Cross Sections for Leptophobic Topcolor Z' Decaying to Top-Antitop*, Eur. Phys. J. **C72** (2012) 2072, arXiv:1112.4928 [hep-ph].

[25] U. Baur, I. Hinchliffe, and D. Zeppenfeld, *Excited Quark Production at Hadron Colliders*, Int. J. Mod. Phys. **A2** (1987) 1285.

[26] U. Baur, M. Spira, and P. M. Zerwas, *Excited Quark and Lepton Production at Hadron Colliders*, Phys. Rev. **D42** (1990) 815–824.

[27] A. J. Larkoski, S. Marzani, G. Soyez, and J. Thaler, *Soft drop*, JHEP **05** (2014) 146, arXiv:1402.2657 [hep-ph].

[28] J. Thaler and K. Van Tilburg, *Identifying Boosted Objects with N-subjettiness*, JHEP **03** (2011) 015, arXiv:1011.2268 [hep-ph].

[29] M. L. Mangano et al., *Physics at a 100 TeV pp Collider: Standard Model Processes*, CERN Yellow Report (2017) no. 3, 1–254, arXiv:1607.01831 [hep-ph].